Effect of Synthesis Conditions on Physiochemical Properties of Lauric Acid Coated Superparamagnetic Iron Oxide Nanoparticles

L. Li[1,2,3], C. W. Leung[4], and P. W. T. Pong[1]

[1]Department of Electrical and Electronic Engineering, The University of Hong Kong, Hong Kong
[2]Department of Chemistry, Tsinghua University, Beijing 100084, China
[3]Research Institute of Tsinghua University, Shenzhen 518055, China
[4]Department of Applied Physics, The Hong Kong Polytechnic University, Hong Kong

Lauric acid coated iron oxide nanoparticles (LAIONPs) is very promising in biomedical applications. Understanding the influences from synthesis processes on physiochemical properties of LAIONPs is very important for their implementations in *in vivo* and *in vitro* studies. Here, the superparamagnetic spherical-shaped LAIONPs samples have been prepared based on coprecipitation method (CP-LAIONPs) and through thermal decomposition using FeO(OH) as iron precursor (TD-LAIONPs), respectively. The effects of different stirring speeds in coprecipitation reaction and different heating profiles in thermal decomposition route on the products properties (including size, mass ratio of surfactants, and saturation magnetization) were revealed. For nanoparticles with similar cores sizes (∼11 nm) obtained from two different synthesis methods, the TD-LAIONPs showed more spherical morphologies, narrower size distributions in both core sizes and hydrodynamic sizes, and stronger magnetic properties than the CP-LAIONPs. In addition, ferromagnetic cubic-shaped LAIONPs with sizes larger than 50 nm could be obtained using another iron precursor in thermal decomposition route. Thus, the synthesis methods and fabrication conditions should be appropriately chosen to obtain LAIONPs with desirable properties for specific purposes.

Index Terms— **Coprecipitation, lauric acid, superparamagnetic nanoparticle, thermal decomposition.**

I. Introduction

MAGNETIC nanoparticles have attracted broad interest in many biomedical areas, such as magnetic resonance imaging (MRI) contrast enhancement, magnetic hyperthermia, cell labeling, drug delivery systems, and magnetic particle imaging [1]. For these applications, the magnetic nanoparticles need to be colloidal stable, biocompatible, and nontoxic. Magnetic iron oxide nanoparticles, mainly constituted by magnetite (Fe_3O_4) or maghemite (γ-Fe_2O_3), emerge as an excellent candidate due to their physiochemical stability, biocompatibility, and low price to produce. To avoid nanoparticles aggregation and to enhance their colloidal stability, iron oxide nanoparticles are usually required to be superparamagnetic and surface coated with biocompatible organic materials. Dextran is one of the organic coating materials proved to be used in commercial magnetic nanoparticles for clinical applications. However, it was reported that the dextran shells on nanoparticles can be broken down due to enzymatic degradation during *in vivo* studies [2]. In addition, the carboxylate surfactants are widely used as coating materials to form steric repulsions between nanoparticles [3]. Lauric acid is one of the classical carboxylate materials, and is already approved for use in pharmaceuticals and food industry, which makes it a very promising coating material for nanoparticles in biomedical applications [4].

Manuscript received March 20, 2015; revised May 4, 2015; accepted June 24, 2015. Date of publication July 1, 2015; date of current version October 22, 2015. Corresponding author: P. W. T. Pong (e-mail: ppong@eee.hku.hk).

Color versions of one or more of the figures in this paper are available online at http://ieeexplore.ieee.org.

Digital Object Identifier 10.1109/TMAG.2015.2451693

The lauric acid coated iron oxide nanoparticles (LAIONPs) have been demonstrated to be biocompatible at low concentration when used in *in vitro* applications [5]. Zaloga *et al.* [6] synthesized the LAIONPs for the adsorption of bovine serum albumin, which shows great potential for clinical applications. Santos *et al.* [7] have fabricated the LAIONPs as a nanosized drug delivery system for amphotericin B, which is a potent antifungal drug. Tietze *et al.* [8] also utilized the LAIONPs to accumulate the chemotherapeutic drug mitoxantrone efficiently in tumors. Sulek *et al.* [9] studied LAIONPs with further peptide coating as the MRI contrast agents. Most of the LAIONPs reported in the literature for biomedical applications are synthesized by coprecipitation (CP-LAIONPs) and subsequent *in situ* coating with lauric acid [5]–[8]. This two-step method inherits the features of coprecipitation, including large-scale production, easiness of manufacturing, cost-effectiveness, but relatively poor uniformity of product sizes. Thermal decomposition method has been widely reported to obtain high-quality magnetic IONPs using different iron precursors and organic surfactants. However, very few studies use the lauric acid as surfactant in thermal decomposition for superparamagnetic nanoparticles [9], thus there is a lack of understanding about the properties of LAIONPs obtained through this route.

Here, we successfully obtained the LAIONPs through an environmental friendly thermal decomposition method (TD-LAIONPs) using nontoxic iron precursor of hydrated iron (III) oxide. We found that the particle size could be tuned by simply changing the heating profiles. The synthesis route was reported to be greatly impactful on the properties of nanoparticle products, such as

aluminum oxide nanoparticles, cobalt ferrite nanoparticles, and so on [10], [11]. To obtain the IONPs with required properties, the synthesis parameters need to be carefully examined and optimized [12], [13]. Therefore, another aim of this paper is to investigate and compare the effects of two different synthesis methods including coprecipitation and thermal decomposition on the physiochemical properties of LAIONPs. Through comparative study on the nanoparticles with similar mean core size (11 nm), the TD-LAIONPs showed narrower size distribution and higher saturation magnetization (weighted by iron oxide) than the ones prepared using coprecipitation method. Our results indicate that the synthesis methods and fabrication conditions should be appropriately chosen to obtain the LAIONPs with desirable properties for specific purposes.

II. Experiments

A. Materials

Ferric chloride hexahydrate ($FeCl_3 \cdot 6H_2O$, $\geqslant$99%), ferrous sulfate heptahydrate ($FeSO_4 \cdot 7H_2O$, $\geqslant$99.0%), sodium hydroxide ($\geqslant$98%), hydrated iron (III) oxide [FeO(OH)], lauric acid ($\geqslant$98%), and 1-octadecene (90%) were purchased from Sigma-Aldrich (USA). All chemicals were used as received.

B. Synthesis of LAIONPs Through Coprecipitation Method

The LAIONPs with three different iron-oxide-core average sizes were obtained through coprecipitation and subsequent *in situ* coating with lauric acid. Typically, aqueous solution with $FeSO_4 \cdot 7H_2O$ and $FeCl_3 \cdot 6H_2O$ at a ratio of 1:2 was added dropwise into prewarmed 1.5 M ammonium hydroxide solution at 80 °C under rigorous magnetic stirring. The black precipitates, indicating the formation of bare iron oxide nanoparticles, were washed by repeated cycles of magnetic attraction and redispersion in DI water, until the pH of solution was adjusted to 7. Then, the fresh precipitates were redispersed in DI water, and heated to 90 °C. Lauric acid was added under continuous stirring for 30 min. The synthesized suspension was precipitated with acetone and washed by repeated cycles of magnetic decanting with acetone and DI water. Using different stirring speeds during the reaction, the LAIONPs with three variable sizes were obtained and named as CP-1 (1200 r/min), CP-2 (800 r/min), and CP-3 (400 r/min).

C. Synthesis of LAIONPs Through Thermal Decomposition Method

The thermal decomposition method to prepare the LAIONPs was carried out in a three-neck flask equipped with condenser, magnetic stirrer, heating mantle, and temperature controller, following William *et al.* protocol with modifications [14]. In a typical synthetic procedure, a mixture of 2 mmol FeO(OH) fine powder, 10 mmol of lauric acid, and 5 g 1-octadecene was stirred and heated to reflux temperature through certain heating procedures, then cooled down to room temperature. The final LAIONPs products were precipitated out of 1-octadecene with acetone by centrifuge, washed several times with 1:2 mixture of chloroform and acetone. Using different heating profiles as shown in Fig. 1, the LAIONPs with three different sizes were obtained and named as TD-1, TD-2, and TD-3.

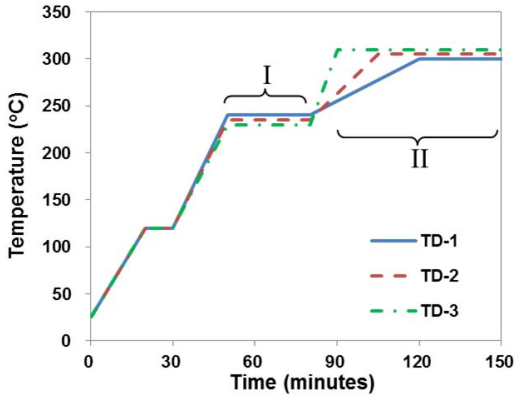

Fig. 1. Heating profiles used in thermal decomposition synthesis for LAIONPs.

D. Characterization of the LAIONPs

Size and morphology of the LAIONPs were observed by transmission electron microscopy (TEM; Philips CM100) and scanning electron microscopy (SEM; Hitachi S-4800 FEG). To prepare samples, diluted drops of the colloidal suspension were allowed to dry slowly on the substrates of carbon-coated copper grids for the TEM observation and silicon wafers for the SEM observation. Average particle diameter, size distributions, and standard derivations were calculated for each LAIONP sample by averaging 60 particles from the TEM images using ImageJ software (NIH). Hydrodynamic sizes of the LAIONPs were examined through dynamic light scattering (DLS) using Malvern Zetasizer 3000 (Malvern, U.K.) at a fixed angle of 90° and temperature 25 °C. Mass ratio of iron oxide composition was determined using thermal gravimetric analysis (TGA, Perkin-Elmer TGA-7). The mass loss of 5–10 mg of power sample was monitored under N_2 gas with sample temperature increasing from 50 °C to 600 °C. The magnetic property of powder sample was measured at room temperature using a vibrating sample magnetometer (VSM) (Lakeshore, VSM 7400). The magnetization was measured over a range of applied field from −10 000 to 10 000 Oe.

III. Results and Discussion

To examine their core size and morphology, the synthesized products were observed under TEM (Figs. 2 and 3). The LAIONPs obtained based on coprecipitation displayed approximately spherical shapes (Fig. 2), and their average diameters are 8.5 ± 1.8 nm (CP-1), 11.3 ± 2.4 nm (CP-2), and 14.2 ± 2.8 nm (CP-3). The mean core size of the LAIONPs decreased when the stirring speed increased during the fabrication processes. This is mainly due to the reduced sizes of bare iron oxide nanoparticles obtained through coprecipitation procedure using increased stirring speed [15], [16]. The reason for this size reduction was suggested to be the anomalous diffusion of particles at higher degree of agitation reduced their growth kinetics, and resulted in the smaller sized particles [15]. Another explanation was proposed to be the energy transferred to the suspension medium, which increased with the increasing

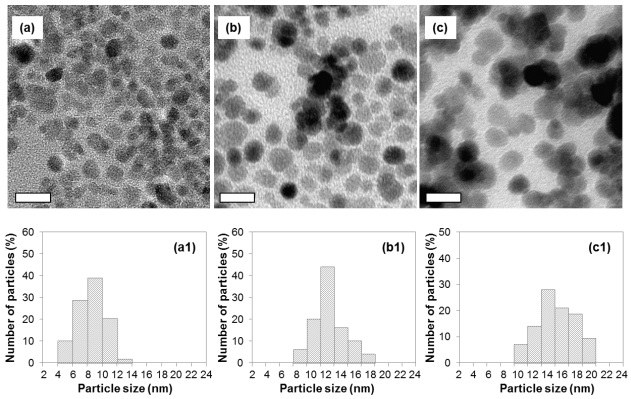

Fig. 2. TEM images of CP-LAIONPs with stirring speed of (a) 1200 r/min, (b) 800 r/min, and (c) 400 r/min. (a1)–(c1) Histogram of particles size distributions in corresponding TEM image. Scale bar: 20 nm.

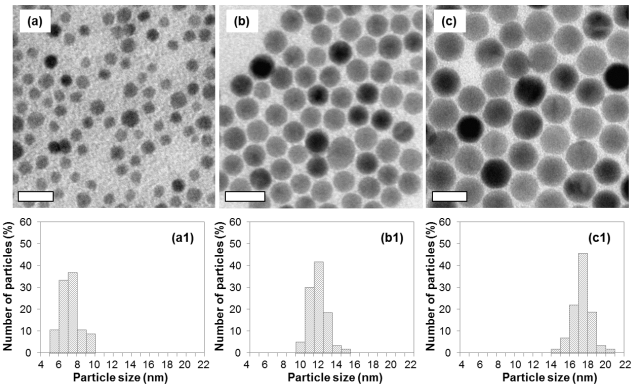

Fig. 3. (a)–(c) TEM images of TD-LAIONPs route by using different heating processes. (a1)–(c1) Histogram of particles size distributions in corresponding TEM image. Scale bar: 20 nm.

stirring rate. The reaction solution was dispersed into smaller droplets thus the particle size was reduced [16].

Compared with the CP-LAIONPs, the TD-LAIONPs of FeO(OH) (Fig. 3) showed more spherical morphologies with average dimensions of 7.2 ± 1 nm (TD-1), 11.4 ± 1 nm (TD-2), and 17.5 ± 1 nm (TD-3). In order to adjust the particle sizes, the seed-mediated growth method is commonly used in thermal decomposition route, but this method usually includes multiple synthesis steps [15], [17]. It was also reported that the particle sizes were tunable by adjusting the molar ratio of organic surfactant and iron precursor [18]. Here, we demonstrated a single-step method to control the particle sizes of LAIONPs from 7 to 17 nm using different heating profiles without changing the amount of the precursors. Although the mechanisms by which monodisperse nanoparticle samples may form are still under debate, it is generally considered that the particles final sizes are affected by nucleation and growth stages [19], [20]. As shown in Fig. 1, faster nucleation rate in phase I (higher temperature of 240 °C) and lower growth temperature in phase II (slower heating rate of 2 °C/min and lower final temperature of 300 °C) resulted in smaller sizes of the LAIONPs in sample TD-1. On the other hand, slower nucleation rate in phase I (lower temperature of 230 °C) and higher growth temperature in phase II (faster heating rate of 8 °C/min and higher final temperature of 310 °C) resulted in larger sizes of LAIONPs in

TABLE I
HYDRODYNAMIC SIZE OF LAIONPS

Samples	Core size (TEM)	Mean diameter (DLS, peak analysis by number)
CP-1	8.5 ± 1.8 nm	20.8 ± 10.6 nm
CP-2	11.3 ± 2.4 nm	25.4 ± 14.8 nm
CP-3	14.2 ± 2.8 nm	31.3 ± 15.4 nm
TD-1	7.2 ± 1.0 nm	11.3 ± 6.3 nm
TD-2	11.4 ± 1.0 nm	15.4 ± 7.5 nm
TD-3	17.5 ± 1.0 nm	21.5 ± 7.8 nm

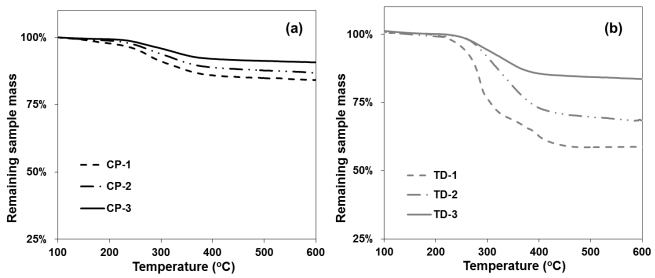

Fig. 4. TGA results of LAIONPs obtained (a) based on coprecipitation method, CP-1, CP-2, and CP-3 and (b) through thermal decomposition route, TD-1, TD-2, and TD-3.

sample TD-3. The similar effects of the decreased nucleation rate and higher growth temperature resulting in larger particles sizes were also found on the $CoPt_3$ and Cu_2ZnSnS_4 nanocrystals obtained through thermal decomposition method [20], [21].

In comparison with the CP-LAIONPs, the TD-LAIONPs displayed narrower size distribution in both core sizes measured on TEM images and hydrodynamic size measured by the DLS technique, as shown in Table I. The hydrodynamic sizes of the CP-LAIONPs are 20.8 ± 10.6 nm for CP-1, 25.4 ± 14.8 nm for CP-2, and 31.3 ± 15.4 nm for CP-3, while the hydrodynamic sizes of the TD-LAIONPs are 11.3 ± 6.3 nm for TD-1, 15.4 ± 7.5 nm for TD-2, and 21.5 ± 7.8 nm for TD-3. The larger hydrodynamic size implies weaker repulsion force from electrostatic/steric interactions or stronger attraction force from van der Waals/ magnetic interactions in the CP-LAIONPs [22]. One possible reason should be due to the smaller surface coverage of surfactants formed on the CP-LAIONPs samples than on the TD-LAIONPs samples, which is evident by TGA results. As shown in Fig. 4, the mass ratios of iron oxide in the CP-LAIONPs samples are 90.7% for CP-3, 86.9% for CP-2, and 84.2% for CP-1, more than the mass ratios of iron oxide in the TD-LAIONPs samples of 83.6% (TD-3), 68.5% (TD-2), and 58.8% (TD-1). Taking CP-2 and TD-2 for example, TD-2 has similar mean core size of 11 nm with CP-2, and both of them are superparamagnetic nanoparticles with zero hysteresis at room temperature (Fig. 5), thus there is no magnetic interaction existing and the attraction force from van der Waals interaction among the nanoparticles could be considered at similar level in these two samples. However, the mass ratio of iron oxide component in CP-2 (86.9%) is higher than in TD-2 (68.5%), indicating a lesser amount of lauric acid surfactants in CP-2. It could result in

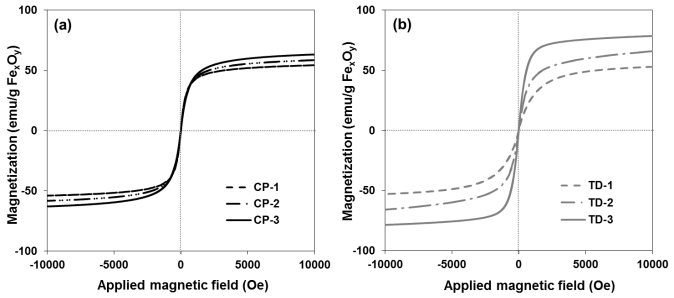

Fig. 5. VSM results of LAIONPs obtained (a) based on coprecipitation method, CP-1, CP-2, and CP-3 and (b) through thermal decomposition route, TD-1, TD-2, and TD-3.

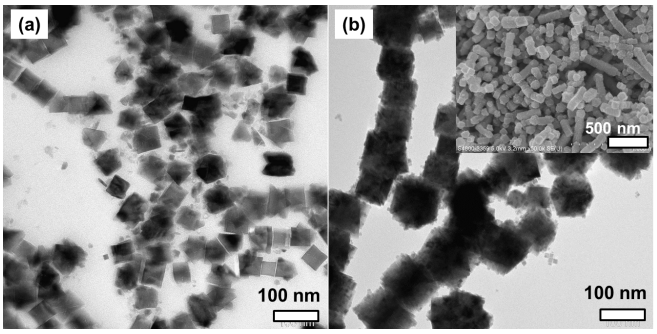

Fig. 6. TEM images of C-LAIONPs obtained from thermal decomposition of iron precursor $Fe(acac)_3$ by using two different heating profiles. (a) LAIONPs nanocubes with smaller mean size of 50 nm. (b) LAIONPs nanocubes with larger mean size of 100 nm. Inset: its corresponding SEM image.

less surface coverage of surfactants on nanoparticles and weaker repulsion force among the nanoparticles in CP-2, thus larger hydrodynamic sizes of the LAIONPs appear in CP-2 than TD-2. The decreased mass ratio of the iron oxide component with the increased particle sizes in the CP-LAIONPs and TD-LAIONPs is because the larger nanoparticles have lower surface-to-volume ratio, and, as such, the binding sites for surfactants provided by total surface area decreased [23].

The magnetic hysteresis loops of the CP-LAIONPs and TD-LAIONPs samples were measured by VSM at room temperature (Fig. 5). All the six LAIONPs samples showed a typical superparamagnetic behavior with no hysteresis, which is beneficial for the biomedical application. Using the TGA results, the saturation magnetization (M_S) value weighted by iron oxide components increased as the particle size increased, which can be observed in both CP-LAIONPs samples (CP-1, 54 emu/g; CP-2, 58 emu/g; and CP-3, 63 emu/g) and TD-LAIONPs samples (TD-1, 53 emu/g; TD-2, 64 emu/g; TD-3, and 78 emu/g). Such a trend is consistent with the reported size effect of magnetic iron oxide particle on its saturation magnetization value in the nanoregime [24], [25]. The M_S value of the TD-LAIONPs sample with the largest core size of 17 nm is close to the bulk value (74 emu/g of γ-Fe_2O_3 and 90 emu/g for Fe_3O_4). For the LAIONPs with similar average core size of 11 nm, the M_S value of TD-2 obtained by thermal decomposition (64 emu/g) was higher than CP-2 obtained by coprecipitation (58 emu/g). This can be explained by the lower crystallinity of nanoparticles formed in CP-2 samples than in TD-2 samples because the reaction temperature in coprecipitation method is limited by the boiling point of water and much lower than the reaction temperature in thermal decomposition method [26]. Poor crystallinity of magnetic IONPs in CP-2 leads to degradation in the magnetic behavior, thus CP-2 showed lower M_S value than TD-2.

Besides the hydrated iron (III) oxide [FeO(OH)] used as iron precursor for TD-LAIONPs (TD-1, TD-2, and TD-3) here, another nontoxic iron precursor $Fe(acac)_3$ was also tested in our one-step thermal decomposition method. Interestingly, the cubic-shaped LAIONPs (C-LAIONPs) were obtained using $Fe(acac)_3$ [instead of FeO(OH)] as iron precursor, benzyl ether (instead of 1-ODE) as high-boiling point solvent, and lauric acid as surfactant. As shown in the TEM images (Fig. 6), the average dimensions of the C-LAIONPs samples can be tuned to be ~50 nm [Fig. 6(a)] or 100 nm [Fig. 6(b)] by controlling the nucleate rate and growth temperature in heating profiles as discussed before. Unfortunately, both of the C-LAIONPs products had dimensions beyond the critical size (~20 nm) of superparamagnetic IONP [27], and displayed a ferromagnetic behavior. Strong magnetic dipole attraction between nanocubes is evident by the formation of chain-like self-assembly pattern of the LAIONPs in the SEM image [Fig. 6(b) (inset)]. Thus, careful study is needed when applying this one-step temperature-paused thermal decomposition route to other iron precursors for the LAIONPs synthesis.

IV. Conclusion

Three CP-LAIONPs samples with average sizes from 8.5 to 14.2 nm were fabricated by changing the stirring speeds during the coprecipitation reaction, while three TD-LAIONPs samples with average diameters from 7.2 to 17.5 nm were obtained by controlling the heating profiles in thermal decomposition. The influence of synthesis conditions on the morphologies, core sizes, hydrodynamic sizes, and magnetic properties of the LAIONPs was revealed. For comparative study on the effects from different synthesis methods, the CP-LAIONPs and TD-LAIONPs with similar average core size (~11 nm) were produced and investigated. In conclusion, all spherical LAIONPs samples exhibited good dispersion in colloidal solution, superparamagnetic behavior, and high iron oxide M_s value above 50 emu/g. Compared with the CP-LAIONPs, the TD-LAIONPs showed more spherical morphologies, narrower size distributions in both core sizes and hydrodynamic sizes, and stronger magnetic properties. In addition, careful study is needed when applying this one-step thermal decomposition route to other iron precursors for the LAIONPs synthesis. For example, the ferromagnetic C-LAIONPs with size larger than 50 nm were obtained when using $Fe(acac)_3$ instead of FeO(OH) in the thermal decomposition routes.

Acknowledgment

This work was supported in part by the University Grants Committee of Hong Kong under Contract AoE/P-04/08, in part by the Seed Funding Program for Basic Research,

in part by the Small Project Funding Program from the University of Hong Kong, in part by ITF Tier 3 Funding under Grant ITS/104/13 and Grant ITS/214/14, and in part by RGC-GRF grant under Grant HKU 704911P. The authors would like to thank F. Chan, EMU, The University of Hong Kong, E. K. S. Cheung, EEE, The University of Hong Kong, and D. Ma, EEE, The University of Hong Kong, for their assistance.

REFERENCES

[1] S. Laurent *et al.*, "Magnetic iron oxide nanoparticles: Synthesis, stabilization, vectorization, physicochemical characterizations, and biological applications," *Chem. Rev.*, vol. 108, no. 6, pp. 2064–2110, 2008.

[2] A. Jordan *et al.*, "Cellular uptake of magnetic fluid particles and their effects on human adenocarcinoma cells exposed to AC magnetic fields in vitro," *Int. J. Hyperthermia*, vol. 12, no. 6, pp. 705–722, Nov./Dec. 1996.

[3] A. K. Gupta and M. Gupta, "Synthesis and surface engineering of iron oxide nanoparticles for biomedical applications," *Biomaterials*, vol. 26, no. 18, pp. 3995–4021, Jun. 2005.

[4] J. L. Kinderlerer, "Degradation of the lauric acid oils," *Int. Biodeterioration Biodegradation*, vol. 33, no. 4, pp. 345–354, 1994.

[5] P. Pradhan, J. Giri, R. Banerjee, J. Bellare, and D. Bahadur, "Cellular interactions of lauric acid and dextran-coated magnetite nanoparticles," *J. Magn. Magn. Mater.*, vol. 311, no. 1, pp. 282–287, 2007.

[6] J. Zaloga *et al.*, "Development of a lauric acid/albumin hybrid iron oxide nanoparticle system with improved biocompatibility," *Int. J. Nanomed.*, vol. 9, no. 1, pp. 4847–4866, 2014.

[7] C. M. B. Santos, S. W. da Silva, L. R. Guilherme, and P. C. Morais, "SERRS study of molecular arrangement of amphotericin B adsorbed onto iron oxide nanoparticles precoated with a bilayer of lauric acid," *J. Phys. Chem. C*, vol. 115, no. 42, pp. 20442–20448, Sep. 2011.

[8] R. Tietze *et al.*, "Efficient drug-delivery using magnetic nanoparticles—Biodistribution and therapeutic effects in tumour bearing rabbits," *Nanomed., Nanotechnol., Biol. Med.*, vol. 9, no. 7, pp. 961–971, Oct. 2013.

[9] S. Sulek *et al.*, "Peptide functionalized superparamagnetic iron oxide nanoparticles as MRI contrast agents," *J. Mater. Chem.*, vol. 21, no. 39, pp. 15157–15162, 2011.

[10] A. Rajaeiyan and M. M. Bagheri-Mohagheghi, "Comparison of sol–gel and co-precipitation methods on the structural properties and phase transformation of γ and α-Al_2O_3 nanoparticles," *Adv. Manuf.*, vol. 1, no. 2, pp. 176–182, 2013.

[11] B. G. Toksha, S. E. Shirsath, S. M. Patange, and K. M. Jadhav, "Structural investigations and magnetic properties of cobalt ferrite nanoparticles prepared by sol–gel auto combustion method," *Solid State Commun.*, vol. 147, nos. 11–12, pp. 479–483, 2008.

[12] M. Mahmoudi, A. Simchi, M. Imani, A. S. Milani, and P. Stroeve, "Optimal design and characterization of superparamagnetic iron oxide nanoparticles coated with polyvinyl alcohol for targeted delivery and imaging," *J. Phys. Chem. B*, vol. 112, no. 46, pp. 14470–14481, 2008.

[13] D. Forge *et al.*, "Optimization of the synthesis of superparamagnetic contrast agents by the design of experiments method," *J. Phys. Chem. C*, vol. 112, no. 49, pp. 19178–19185, 2008.

[14] W. Y. William, J. C. Falkner, C. T. Yavuz, and V. L. Colvin, "Synthesis of monodisperse iron oxide nanocrystals by thermal decomposition of iron carboxylate salts," *Chem. Commun.*, vol. 20, no. 20, pp. 2306–2307, 2004.

[15] S. Sun and H. Zeng, "Size-controlled synthesis of magnetite nanoparticles," *J. Amer. Chem. Soc.*, vol. 124, no. 28, pp. 8204–8205, 2002.

[16] J. Sun *et al.*, "Synthesis and characterization of biocompatible Fe_3O_4 nanoparticles," *J. Biomed. Mater. Res. A*, vol. 80, no. 2, pp. 333–341, 2007.

[17] Y. Yamamoto *et al.*, "Size dependence study on magnetic heating properties of superparamagnetic iron oxide nanoparticles suspension," *J. Appl. Phys.*, vol. 116, no. 12, p. 123906, 2014.

[18] W. W. Yu, J. C. Falkner, C. T. Yavuz, and V. L. Colvin, "Synthesis of monodisperse iron oxide nanocrystals by thermal decomposition of iron carboxylate salts," *Chem. Commun.*, vol. 20, no. 20, pp. 2306–2307, 2004.

[19] L. Zhang, R. He, and H.-C. Gu, "Synthesis and kinetic shape and size evolution of magnetite nanoparticles," *Mater. Res. Bull.*, vol. 41, no. 2, pp. 260–267, 2006.

[20] A. Khare, A. W. Wills, L. M. Ammerman, D. J. Norris, and E. S. Aydil, "Size control and quantum confinement in Cu_2 $ZnSnS_4$ nanocrystals," *Chem. commun.*, vol. 47, no. 42, pp. 11721–11723, 2011.

[21] E. V. Shevchenko *et al.*, "Study of nucleation and growth in the organometallic synthesis of magnetic alloy nanocrystals: The role of nucleation rate in size control of $CoPt_3$ nanocrystals," *J. Amer. Chem. Soc.*, vol. 125, no. 30, pp. 9090–9101, Jul. 2003.

[22] J. Lim, S. P. Yeap, H. X. Che, and S. C. Low, "Characterization of magnetic nanoparticle by dynamic light scattering," *Nanosc. Res. Lett.*, vol. 8, no. 17, pp. 1–14, 2013.

[23] J. K. Bailey, C. J. Brinker, and M. L. Mecartney, "Growth mechanisms of iron oxide particles of differing morphologies from the forced hydrolysis of ferric chloride solutions," *J. Colloid Interf. Sci.*, vol. 157, no. 1, pp. 1–13, 1993.

[24] M. Mahdavi *et al.*, "Synthesis, surface modification and characterisation of biocompatible magnetic iron oxide nanoparticles for biomedical applications," *Molecules*, vol. 18, no. 7, pp. 7533–7548, 2013.

[25] A. Demortiere *et al.*, "Size-dependent properties of magnetic iron oxide nanocrystals," *Nanoscale*, vol. 3, no. 1, pp. 225–232, 2011.

[26] G. Rana and U. C. Johri, "Correlation between the pH value and properties of magnetite nanoparticles," *Adv. Mater. Lett.*, vol. 5, no. 5, p. 280, 2014.

[27] L. Li, C. Leung, and P. Pong, "Magnetism of iron oxide nanoparticles and magnetic biodetection," *J. Nanoelectron. Optoelectron.*, vol. 8, no. 5, pp. 397–414, 2013.